AgEcon SEARCH
RESEARCH IN AGRICULTURAL & APPLIED ECONOMICS

The World's Largest Open Access Agricultural & Applied Economics Digital Library

This document is discoverable and free to researchers across the globe due to the work of AgEcon Search.

Help ensure our sustainability.

Give to AgEcon Search

AgEcon Search
http://ageconsearch.umn.edu
aesearch@umn.edu

*Papers downloaded from **AgEcon Search** may be used for non-commercial purposes and personal study only. No other use, including posting to another Internet site, is permitted without permission from the copyright owner (not AgEcon Search), or as allowed under the provisions of Fair Use, U.S. Copyright Act, Title 17 U.S.C.*

18 Upscaling Water Productivity in Irrigated Agriculture Using Remote-sensing and GIS Technologies

Wim Bastiaanssen,[1] Mobin-ud-Din Ahmad[2] and Zubair Tahir[3]
[1] *International Institute for Aerospace Survey and Earth Sciences, Enschede, The Netherlands;* [2] *International Water Management Institute, Colombo, Sri Lanka;* [3] *International Water Management Institute, Lahore, Pakistan*

Abstract

Reliable information on water depletion for agricultural production is much needed when freshwater resources are getting scarcer. This is the case in the irrigated Indus basin. Despite their importance, data required to monitor the productivity of the land and water resources over vast areas are usually not available or accessible. Satellite measurements from the National Oceanic and Atmospheric Adminstration (NOAA) weather satellite are combined in this study with ancillary *in situ* data into a geographic information system (GIS). Remote-sensing measurements are converted to crop yield, to actual evapotranspiration and, indirectly, to net groundwater use. The GIS data consist of canal-water deliveries and rainfall records. For each of the canal commands, the productivity of water is calculated. Large variability in the data is found from the different canal commands in the Indus basin. It is concluded that water productivity is controlled more by crop yields than by the water input. The spatial variability of productivity per unit water diverted is greater than per unit depleted. This can be ascribed to wide variations in the relationship between canal-water supply and actual evapotranspiration. This is an issue covered by classical irrigation efficiencies. Upscaling of water productivity for the Indus basin was achieved by aggregating the various canal command areas from the upstream end of the system downwards. The results show that the productivity of water tends to a constant value at a spatial scale of 6 million ha and higher. At that scale, water diversion and water depletion are equal, which implies that groundwater systems, to a large extent, regulate losses and reuse of water resources. The Indus basin is an example of substantial groundwater recycling and this needs to be taken into account in analytical frameworks of water productivity.

Introduction

When freshwater resources are getting scarcer, such as in the irrigated Indus basin, it is necessary to have an accurate description of the depletion of the water resource as a result of agricultural production. Frameworks for the formulation and assessment of water productivity have been developed by Molden *et al.* (1998) and Seckler *et al.* (Chapter 3, this volume), and have been used in water-management studies (e.g. Droogers and Kite, 1999).

Water-management techniques often focus on 'saving' water at field level, but, in water-scarce conditions, water is diverted at one

© CAB International 2003. *Water Productivity in Agriculture: Limits and Opportunities for Improvement* (eds J.W. Kijne, R. Barker and D. Molden)

place and used at another. It is, therefore, of extreme importance to gain an insight into the efficiencies and productivities at larger scales. Traditional field surveys and field-scale water-balance measurements cannot give a comprehensive description of the water flows at the regional scale. Processes, such as recharge, capillary rise and groundwater extractions, are difficult to measure or estimate for subsystems. These water terms are mentioned in particular, as they are reflected in the processes of water recycling. However, information on crop acreage, yields and canal-water deliveries is also difficult to obtain, as actual canal operation may differ substantially from the planning and design discharges.

Lack of data required for monitoring the productivity of the land and water resources, especially over vast irrigation schemes and river basins, can often hamper the application and understanding of the water-productivity framework. The aim of this chapter is to demonstrate how remote-sensing and geographic information system (GIS) tools can help in assessing water productivity and how productivity varies with spatial scale.

Hydrological Approach

The soil-water balance and crop-production values form the basis for the water-productivity analysis. The soil-water balance relates total supply to total consumption and has a storage term for cases when inflow and outflow are not balanced (see also Fig. 18.1).

$$\Delta S = (P + I_{cw} + I_{tw} + q^{\uparrow}) - (ET_a + q^{\downarrow}) \quad \text{(mm)} \qquad (18.1)$$

where ΔS is the storage change, P is precipitation, I_{cw} is canal-water supply, I_{tw} is groundwater supply through tube wells, $q^{\uparrow}$ is capillary rise, ET_a is the actual evapotranspiration and $q^{\downarrow}$ is the recharge. Since several terms of Equation 18.1 are difficult to quantify, the three groundwater terms are taken together:

$$NGW = I_{tw} + q^{\uparrow} - q^{\downarrow} \quad \text{(mm)} \qquad (18.2)$$

where NGW is the net groundwater use, i.e. the extractions of groundwater minus the net recharge. NGW represents the net withdrawal of groundwater, which is important for the sustainability analysis. The recharge $q^{\downarrow}$ comprises the return flow from tube-well irrigation, I_{tw}, but can also arise from precipitation, P, and canal-water irrigation, I_{cw}. After combining Equations 18.1 and 18.2, the simplified water-balance equation is:

$$\Delta S = P + I_{cw} + NGW - ET_a \quad \text{(mm)} \qquad (18.3)$$

For the current case study in the Indus basin, P is taken from rain gauges, I_{cw} from flow records and ET_a from remote sensing. The two unknowns are then ΔS and NGW. If, in addition, the storage changes are ignored, which is not correct in all canal command areas, NGW remains as the residual term of the water balance. The storage changes depend on groundwater-table fluctuations, which in some cases can be as much as 100 mm year^{-1} (see Ahmad and Bastiaanssen, 2003). A sufficient number of piezometric readings was not available to estimate ΔS in a systematic manner across the entire Indus basin. Because of this limitation, ΔS was disregarded, as is usually done in hydrological studies for longer time periods.

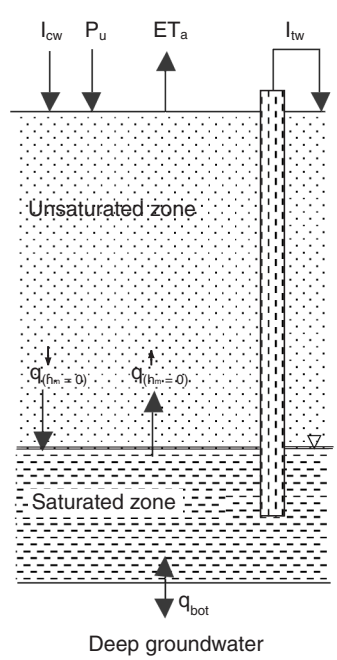

Fig. 18.1. Schematic presentation of the soil-water balance.

Hydrological Results

Data on precipitation and canal-water supply were taken from Habib *et al.* (1999) and from Tahir and Habib (2000). The Indus basin comprises 44 canal command areas, some of which have incomplete data and were, therefore, not further considered in this study. The data on canal-water supply per unit culturable command area show a variation of 40 to 830 mm during the rabi (dry winter) season (Fig. 18.2). This suggests a very non-uniform distribution of irrigation water across the Indus basin during the dry winter season. Similar heterogeneity in canal-water supply was found for kharif (wet summer). These large deviations may result, in part, from measurement and interpretation errors in the main canals, as flows through these huge irrigation canals are not easy to measure accurately. The numbers used in this study for canal command areas, with complete data sets for all water-balance terms, are presented in the Appendix.

Actual evapotranspiration data are taken from Bastiaanssen *et al.* (2002), who based their analysis on remotely sensed data. Raw data from the National Oceanic and Atmospheric Administration – Advanced Very High Resolution Radiometer satellite (NOAA-AVHRR) were used. The surface energy-balance algorithm for land (SEBAL) has been applied to convert the raw satellite data into broadband surface albedo, vegetation index and surface temperature. The major objective of SEBAL is to explore the range of: (i) surface albedo values for describing net radiation; (ii) vegetation indices to assess the variability of soil heat flux; and (iii) surface temperatures for estimating sensible heat flux. The energy-balance equation is used to compute actual evapotranspiration from the energy left for the latent heat flux:

$$LE_{24} = R_{n24} - H_{24} \qquad (Wm^{-2}) \qquad (18.4)$$

where LE_{24} is the 24 h latent heat flux associated with evapotranspiration, R_{n24} is the 24 h net radiation and H_{24} is the 24 h sensible heat flux. The soil heat flux on a 24 h basis is usually small and can be ignored. LE_{24} can be converted into actual evapotranspiration (mm day^{-1}) from the energy required to vaporize 1 kg of water at a given temperature. Equation

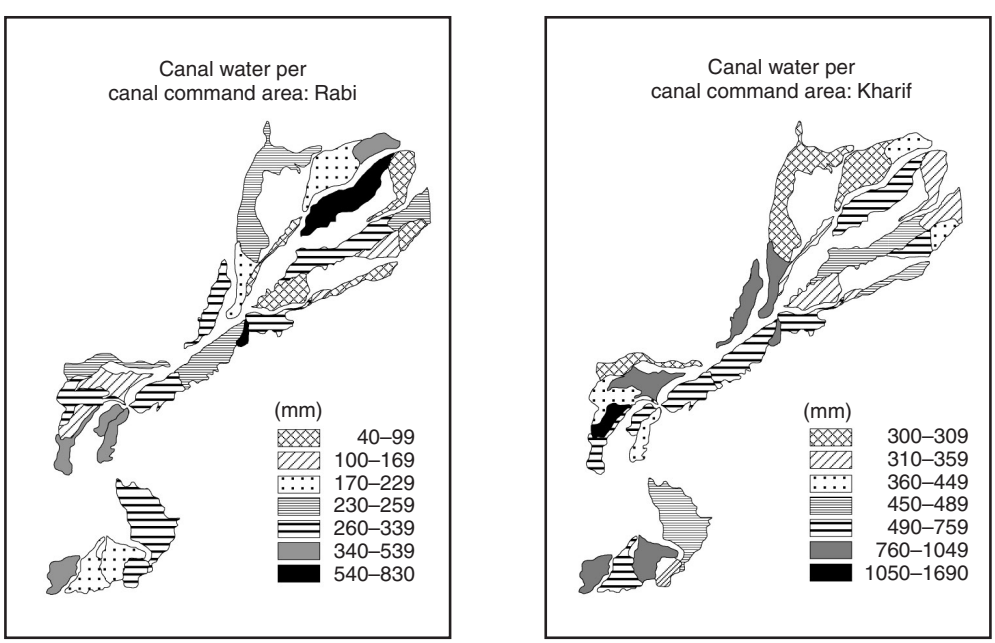

Fig. 18.2. Canal-water use in rabi (1993/94) and kharif (1994) for the Indus basin based on secondary data.

18.4 was used to compute the actual evapotranspiration for cloud-free NOAA images acquired during 20 different days throughout an annual cycle. Individual day results were temporally integrated by preserving the evaporative fraction between two successive satellite acquisition days. The evaporative fraction on a daily time basis is equal to LE_{24}/R_{n24}. This energy partitioning was fixed until the next available AVHRR image. Since net radiation changes considerably due to cloud cover that may arise during satellite flyover days, day-to-day variations of R_{n24} have been taken into account to compute LE_{24} from the temporally preserved LE_{24}/R_{n24} fraction. The Indus basin was divided for this purpose into five climatic zones, and daily global radiation (short-wave radiation reaching the land surface) was computed for every climatic zone.

Figure 18.3 shows the map of annual actual evapotranspiration. Validation in the Indus basin was realized through the application of the well-calibrated field-scale transient moisture-flow model SWAP (Sarwar *et al.*, 2000), *in situ* Bowen ratio measurements (Ahmad *et al.*, 2002) and water-balance residual analyses for an area of 3 million ha. The accuracy of assessing time-integrated evaporative depletion was found to vary from 0.3% at field scale to 4.5% at the regional scale of 3 million ha.

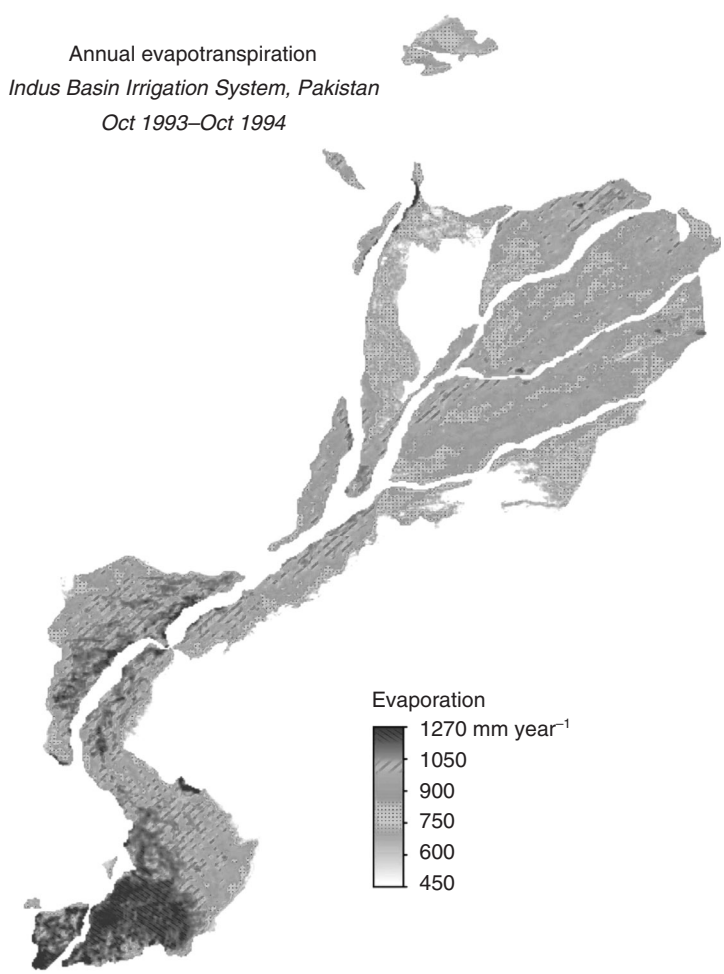

Fig. 18.3. Annual actual evapotranspiration determined from NOAA-AVHRR satellite data using the physically based SEBAL model.

Actual evapotranspiration during the rabi was, on average, 350 mm, while kharif had a total consumption of 620 mm. The spatial variation is again – as for canal-water supply – very high, with annual evapotranspiration values ranging from 450 to 1270 mm year^{-1}!

Water supply to the cropped area can come from three difference sources, i.e. canal irrigation, I_{cw}, groundwater irrigation, I_{tw}, and net precipitation, P_n (gross precipitation P minus interception losses P_i and surface runoff). For the sustainability of irrigation systems, it is important to estimate the extent to which irrigated agriculture depends on groundwater resources. The groundwater–resource ratio, ξ , is defined as the ratio of groundwater irrigation, I_{tw}, to the total inflow from all sources:

$$\xi = I_{tw}/(I_{cw} + I_{tw} + P_n) \qquad (-) \qquad (18.5)$$

A map of the groundwater–resource ratio ξ is shown in Fig. 18.4. It demonstrates that there is little contribution of groundwater during kharif and a relatively significant amount of groundwater use during the dry rabi season (the rainfall in many areas varies from 25 to 50 mm). During rabi, some areas rely for 80% of their water resources on groundwater.

Crop Yield

Crop yield is a major input in water-productivity frameworks. Crop-yield information is classically collected through field surveys. This is a laborious activity, especially when one has to deal with vast areas. To aid the ground sampling and to swiftly obtain an overall picture of the crop development, a remote-sensing model for crop-yield prediction was developed and applied (Bastiaanssen and Ali, 2003). This model is based on Monteith's equation for biomass production, which reads in its simplest form as:

$$B_{io} = \text{APAR}\ \varepsilon \qquad (\text{kg m}^{-2}\ \text{day}^{-1}) \qquad (18.6)$$

where B_{io} (kg m^{-2} day^{-1}) is the biomass production, APAR (MJ m^{-2}) is the absorbed photosynthetic active radiation and ε (kg MJ^{-1}) is the light-use efficiency. Incoming solar radiation and light interception by leaves control APAR. Solar radiation was computed from the actual hours of sunshine, and the leaf presence from the normalized difference vegetation index (NDVI), being derived from the NOAA-AVHRR sensor. The light-use efficiency ε depends not only on the type of crop (C_3 or C_4), but also

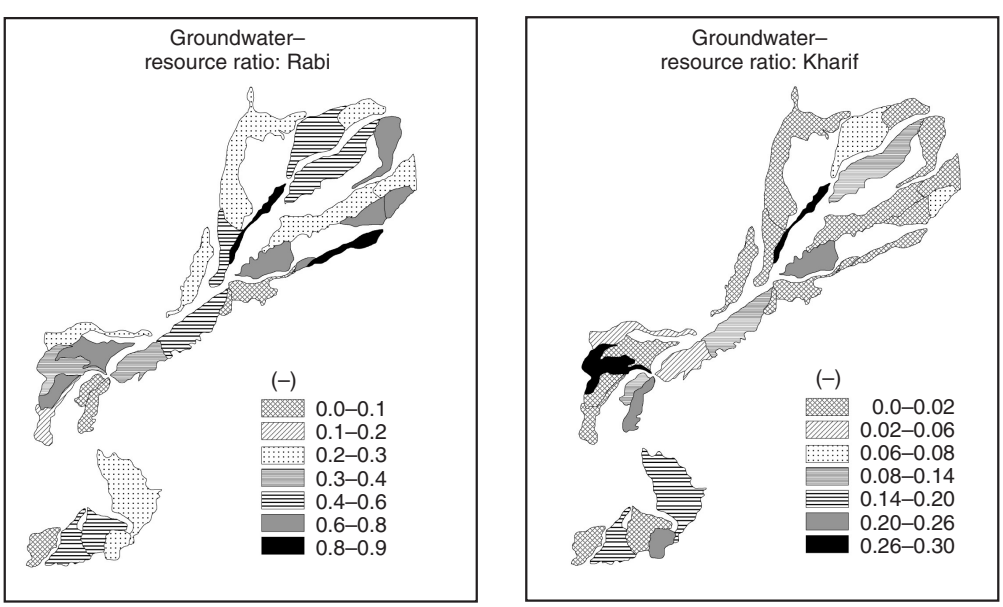

Fig. 18.4. Groundwater–resource ratio (fraction net groundwater use/total water resources available) for canal command areas in rabi (1993/94) and kharif (1994).

on the soil-moisture availability, which affects leaf water potential. Moisture stress reduces the light-use efficiency, and this feedback was taken into account by incorporating the evaporative fraction (LE_{24}/R_{n24}) into the light-use efficiency. The biomass production rates for single NOAA acquisition days were further integrated in time by considering day-to-day variation of cloud cover, which affects APAR because clouds reflect and scatter solar radiation. The light-use efficiency ε was made quasi-variable by adjusting the value between consecutive NOAA images.

Remote-sensing estimates of crop yield have been validated against secondary data collected by the Agriculture Department of Pakistan. The validation revealed a root mean square error of 525, 616, 551 and 13,484 kg ha^{-1} for wheat, rice, cotton and sugarcane yield, respectively. The deviation between secondary data and remote-sensing data shows that the yield of wheat, rice and sugarcane can be mapped for approximately 80% of the cases within the 95% confidence levels of the secondary field data. On average, crop yields in Pakistan are on the lower side. The yields are 2276, 1756, 1293 and 47,929 kg ha^{-1} for wheat, rice, cotton and sugarcane, respectively. A comparison with the study of Hussain *et al.* (2000), who collected crop-cutting experimental data in Sindh, confirmed the wheat yields to be low in Sindh. In Fig. 18.5, yields of wheat, cotton and rice are presented for 26 out of the 44 canal commands. The canal command areas are numbered from the upstream to the downstream end. It is evident that, except for wheat, location in the basin does not significantly affect yields.

Water Productivity

One of the first issues in water-productivity data is to identify which 'crop' and which 'drop' are referred to. To differentiate between water productivity per unit depleted and per unit canal-water supply makes sense, as the former describes how productively water that leaves the basin is used, whereas the latter illustrates the return from canal-management efforts and irrigation-sector investments.

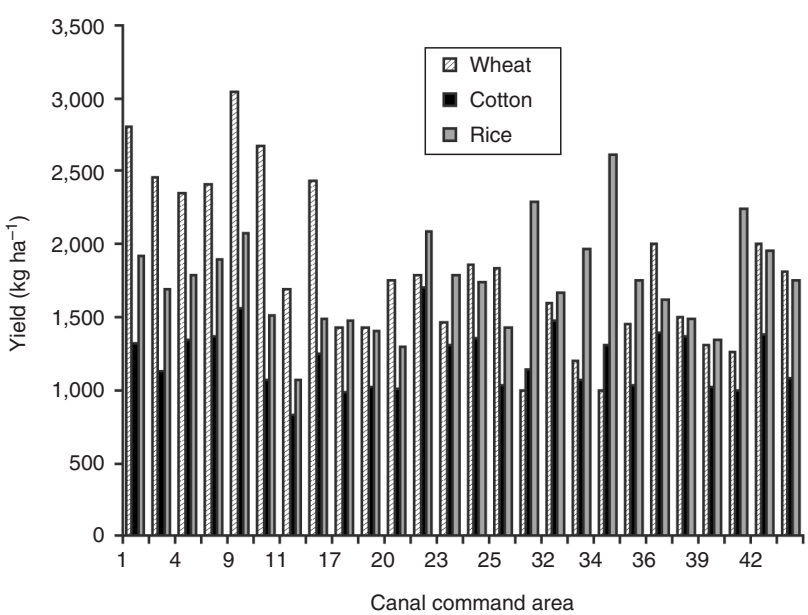

Fig. 18.5. Canal command area yield data for wheat, cotton and rice. The yield data have been computed from NOAA-AVHRR data.

Molden *et al.* (1998) suggested defining water productivity per unit diverted irrigation supply, the latter meaning '*surface irrigation water diverted to the command area plus net removals from groundwater*' (writers' italics). There are reasons why we believe that the use of 'unit canal-water supply' in the denominator may have some advantages for the Indus basin:

- The irrigation manager is responsible for canal-water supply and prefers to understand the impact of the expensive irrigation infrastructure. Groundwater management is usually delegated to institutions other than the irrigation departments.
- Adding together water flows originating from different sources (P, I_{cw}, I_{tw}) prevents the study of the impact of separate sources. In particular, the important role of groundwater in respect of water productivity gets hidden if it is included in the diverted water.

We propose using the following set of definitions:

$$WP_{ETa} = Y_a/ET_a \quad (\text{kg m}^{-3}) \quad (18.7)$$

$$WP_{Icw} = Y_a/I_{cw} \quad (\text{kg m}^{-3}) \quad (18.8)$$

$$WP_{\$} = GVP/I_{cw} \quad (\text{US\$ m}^{-3}) \quad (18.9)$$

where Y_a (kg ha^{-1}) is the actual crop yield and GVP (US\$ kg^{-1}) is the gross value of production. GVP is computed from the crop production of every crop, its market price and its acreage. The indicator $WP_{\$}$ is especially suitable as it comprises the total production of different crops. Also, it can be used in the comparison with water-productivity values of other users, such as fish production, ecosystems, etc.

Y_a and ET_a raster data from satellites can be easily combined to make crop-specific evaluations of WP_{ETa}; this is not straightforward for Y_a/I_{cw}, as crop-specific I_{cw} data are seldom available. Hence, WP_{ETa} has the advantage that it can be used to make crop-specific evaluations. Table 18.1 contains an overview of the basin-wide crop-specific productivity values. It shows that sugarcane and cotton have higher water consumption than rice because of their longer growing period. Cotton has the lowest WP_{ETa} values and sugarcane the highest. However, the use of world market prices of agricultural products for 1994 shows that cotton is more economically productive than rice and wheat. This, by itself, shows that evaluating agricultural production and water-resources depletion is not straightforward.

With data on crop yield, actual evapotranspiration and canal-water flow available in the GIS database, it became feasible to compute WP_{ETa} and WP_{Icw}. The case of wheat is given as an example (Fig. 18.6). WP_{ETa} varies from 0.2 to 0.8 kg m^{-3}, which is really a low value. A literature search on WP_{ETa} for wheat showed an average value of approximately 1.0 kg m^{-3}; hence, Pakistan is performing poorly in terms of WP_{ETa}, as the whole range is less than the worldwide average. The WP_{ETa} trend in Fig. 18.6 shows that the response of wheat yield to evaporation is not constant; the value for WP_{ETa} increases with higher yields ($R^2 = 0.83$). The obvious conclusion, then, is that wheat with a higher yield is more efficient in terms of water depletion. This is worth exploring further in future studies.

Table 18.1. Average output in terms of physical and economical production per unit water depleted in the Indus basin during rabi 1993/94 and kharif 1994.

Crop	Evapotranspiration (mm)	Crop yield (kg ha^{-1})	Productivity per unit consumed (kg m^{-3})	GVP per unit consumed (US\$ m^{-3})
Cotton	579	1,293	0.22	0.43
Rice	414	1,756	0.42	0.13
Wheat	357	2,276	0.64	0.10
Sugarcane	965	47,929	4.97	–

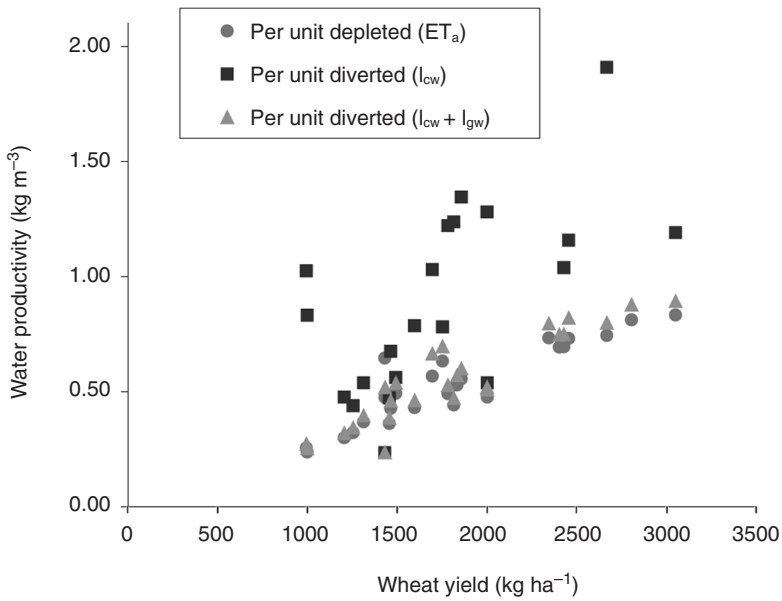

Fig. 18.6. Relationship between water and land productivity for a wheat crop across the Indus basin. Every point represents one canal command area.

WP_{Icw} is higher than WP_{ETa} because ET_a exceeds I_{cw} during the dry winter season. The spatial variability of WP_{Icw} is more than for WP_{ETa}, because ET_a and I_{cw} have a weak relationship due to unequal canal-water distribution throughout the basin (see Fig. 18.2). This brings us to the relationship between ET_a and I_{cw}, which is addressed in the classical irrigation-efficiency concept (e.g. Israelsen, 1950; Keller *et al.*, 1996; Seckler *et al.*, Chapter 3, this volume) as:

$$E_c = (ET_a - P_{net})/I_{cw} \times 100 \qquad (18.10)$$

where the numerator represents the net irrigation requirements and the denominator the canal-water supply. When the efficiency, E_c, is lower than 100%, water that is not evaporated from moist soil or transpired by crops is considered as lost in the classical efficiency concept. This may be true if water that is drained from irrigation schemes flows out of the basin or is no longer available for further use by any other means. In most cases, however, drainage water rejoins the river downstream of an irrigation system.

In the absence of a surface-water drainage system, this 'lost' water stays in the system as groundwater. Irrigation systems such as in the Indus basin are underlain by a productive aquifer with high permeability, and here groundwater is transferred laterally and pumped up by shallow and deep tube wells. If this water is reused in an irrigation system, classical efficiency is not a suitable indicator of water productivity. Thus, canal water 'lost' from one irrigation command area may be reused in another.

Classical irrigation efficiencies were calculated for a set of canal commands for both rabi and kharif seasons to demonstrate how: (i) groundwater use has surprising effects on the irrigation efficiency; and (ii) ET_a relates to I_{cw} . Figure 18.7 shows that, in the wet summer kharif season, E_c ranges between 50 and 200%. The map shows that canal command areas with $E_c > 100\%$ can be found next to command areas with $E_c < 100\%$. This suggests that there is a net groundwater movement in the direction of the command area with the highest efficiency. Unfortunately, appropriate piezometric data were not available to verify these flow directions. But, if $ET_a >> (P + I_{cw})$, it is obvious that groundwater is an important source of irrigation.

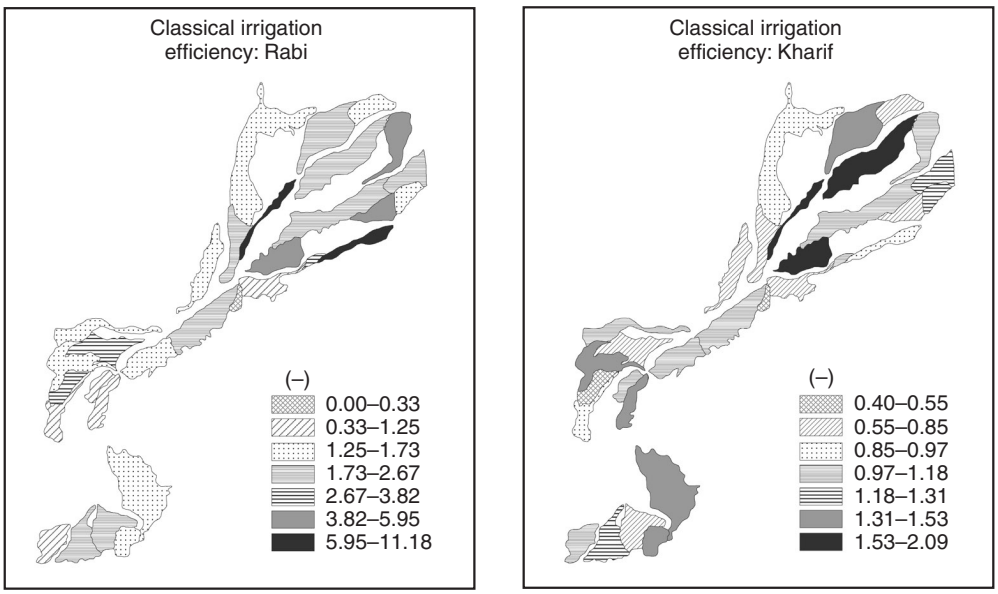

Fig. 18.7. Classical irrigation efficiencies for canal command areas in rabi (1993/94) and kharif (1994). The values are given as a fraction.

By comparing the situation in the two seasons, it appears that command areas having a low E_c in kharif – because precipitation P and canal water I_{cw} far exceed the actual crop evapotranspiration ET_a – respond with $E_c > 100\%$ during the rabi season. This is feasible if kharif water is carried over to the rabi season through soil moisture and groundwater storage mechanisms. Hence, Fig. 18.7 shows that recycling of water is a very important issue in the Indus basin, not only between adjoining command areas, but also between successive growing seasons. Thus, groundwater acts as a storage mechanism and a mediator for making canal operations more effective.

Spatial-scale Issues

How do the water productivity and efficiency change with scale? Our GIS database allowed us to aggregate various canal command areas. This has been done in the upstream to downstream direction, which allowed us to study the productivity at different spatial scales. The hydrological data were combined first and weighted according to the area, i.e. mixing-cell approach. Thereafter, the productivity was recalculated assuming that one is dealing with a unified and larger canal command area, instead of a mosaic of separated canal command areas. The smallest scale is 43,000 ha and the largest scale for a total of 32 combined canal command areas became 11.6 million ha. The total size of all canal command areas in the Indus basin is larger, but not all of them could be included, due to missing data. The wheat crop in the rabi season was chosen because it is the dominant winter crop and most canal water is used for the irrigation of wheat. Figure 18.8, which is a plot of the upscaled water productivity of wheat production during rabi 1993/94, shows two very important phenomena:

- WP_{Icw} has greater spatial scale variability than WP_{ETa}.
- WP_{Icw} and WP_{ETa} tend to have the same value at increasing scales.

The highest water productivity in the Indus basin occurs in smaller canal command areas, especially where the groundwater-resource ratio is high. But, as can be seen in Fig. 18.8, low water-productivity

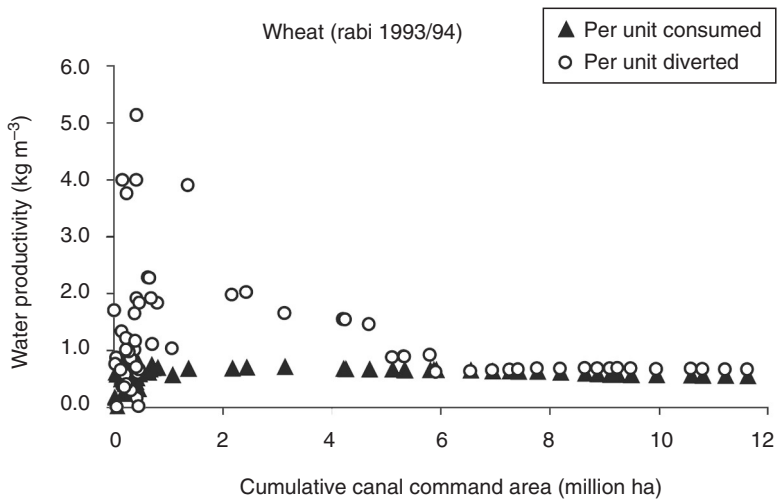

Fig. 18.8. Upscaling of water productivity over the canal command areas in the Indus basin system for the dry winter season, when wheat is predominantly cultivated.

values are also found at this smaller scale. Figure 18.8 shows that PW_{Icw} decreases from 2.0 kg m^{-3} at a scale of 2.0 million ha to 1.0 kg m^{-3} at the 6 million ha scale. These results arise from merging the more fertile soils with a high yield in Punjab in the upstream part of the basin, with the downstream areas receiving less canal water during rabi and being prone to salinity in Sindh.

Water-management interventions and water-saving techniques should therefore focus more on reducing the wide range in WP_{Icw} values at scales between, say, 10,000 to 1 million ha, and not aim to promote changes in one (small) area within the basin. An important conclusion from this work is that increasing WP_{Icw} in a poorly performing canal command area comes at the cost of highly productive systems elsewhere in the region. But it will result in less fluctuation of WP_{Icw} at a lower scale and reduces the scale below which variability becomes insignificant. One of the targets in water-resources management is to obtain the averages of WP_{ETa} = 0.55 and WP_{Icw} = 0.66 kg m^{-3} at the smallest possible scale, i.e. the scale above which no further changes in the values are likely to occur (correlation length in geostatistics).

Conclusions

Water productivity can be expressed per unit water diverted and per unit water depleted. Since actual crop yield and actual evapotranspiration both depend on plant physiological processes – stomata need to open for carbon inhalation and vapour exhalation – the productivity per unit depleted shows less variability than the productivity per unit diverted. The relationship between diversion and depletion is complex and not clear beforehand. It is demonstrated in this chapter that the ratio of crop yield to evapotranspiration is not conservative and there is some scope for improving productivity per unit depleted, by enhancing physical yield per unit land area.

The biggest challenge, though, is to increase the productivity per unit of water diverted. The results reveal that a significant variability exists due to variations in the classical irrigation efficiency. The variations average out if one moves to a larger scale. This can only be explained hydrologically if groundwater recycling occurs as a predominant process. Water budgets demonstrate that net groundwater use is a key component of the water balance. Productivity of water per unit consumed and per unit diverted

become equal at a scale of 6 million ha, which proves that water in the Indus basin is not lost but is used by evaporative depletion elsewhere in the system. A significant transfer of water was detected from the wet summer season to the dry winter season. But groundwater may also flow to adjoining canal command areas. Piezometric information is required to verify this hypothesis.

The impact of small-scale interventions, such as alternate wet–dry phases in rice production, zero tillage, micro-water harvesting, etc., can help improve the local water productivity. There is, however, a possibility that they adversely affect water productivity elsewhere and may further enhance spatial differences in water productivity. Therefore, we recommend narrowing the amplitude of water productivity. That will ultimately lead to a smaller scale above which the average water productivity in the basin stabilizes. Interventions should start in the areas with the lowest water productivity.

Significant progress has been made in the development of frameworks for irrigation efficiency, performance ratios, etc. It is felt that carry-over groundwater from neighbouring irrigation schemes and from the preceding season needs to be more explicitly addressed in these analytical water-productivity frameworks.

This work has demonstrated how affordable images, such as NOAA-AVHRR or from alternative sensors, can help in providing a quick scan of parameters necessary for water-productivity assessment. More research needs to be done on the assessment of soil water-storage changes. Satellite data have been used to determine crop occurrence, actual evapotranspiration by crops, crop yield and, indirectly, net groundwater use. This helps in environments where data are not present or are difficult to access. Coarse images, such as NOAA, are suitable for getting an overall impression at scheme level. Smaller areas or specific crop types would require finer-resolution images, such as those available from Landsat and the Advanced Spaceborne Thermal Emission and Reflection Radiometer.

Acknowledgements

The authors wish to express their gratitude to the Punjab Irrigation and Drainage Authority (PIDA), Pakistan Meteorological Department (PMD), Water and Power Development Authority (WAPDA) and the Directorate of Economic and Marketing of the Provincial Agriculture Department for making available the required information.

References

Ahmad, M.D. and Bastiaanssen, W.G.M. (2003) Retrieving soil moisture storage in the unsaturated zone from satellite imagery and bi-annual groundwater table fluctuations. *Irrigation and Drainage Systems* (in press).

Ahmad, M.D., Bastiaanssen, W.G.M. and Feddes, R.A. (2002) Sustainable use of groundwater for irrigation: a numerical analysis of the subsoil water fluxes. *ICID Journal for Irrigation and Drainage* 51(3), 227–241.

Bastiaanssen, W.G.M. and Ali, S. (2003) A new crop yield forecasting model based on satellite measurements applied across the Indus basin, Pakistan. *Journal of Agriculture, Ecosystems and Environment* 94(3), 321–340.

Bastiaanssen, W.G.M., Ahmad, M.-ud-D. and Chemin, Y. (2002) Satellite surveillance of evaporative depletion across the Indus basin. *Water Resources Research* 38(12), 1273–1282.

Droogers, P. and Kite, G.F. (1999) Water productivity from integrated basin modeling. *Irrigation and Drainage Systems* 13, 275–290.

Habib, Z., Tahir, Z. and Khan, A.R. (1999) Across-the-basin-analysis of water and land utilization using spatio-temporal information techniques emphasize the need for integrated resources management. In: Musi, Fritsch and Pereira (eds) *Proceedings of the 2nd Inter-Regional ICID Conference on Water and Environment, Lausanne, September 1999.*

Hussain, I., Marikar, F. and Jehangir, W. (2000) *Productivity and Performance of Irrigated Wheat Farms Across*

Canal Commands in the Lower Indus Basin. IWMI Research Report 44, International Water Management Institute, Colombo, Sri Lanka.

Israelsen, O.W. (1950) *Irrigation Principles and Practices*, 2nd edn. John Wiley & Sons, New York.

Keller, A., Keller, J. and Seckler, D. (1996) *Integrated Water Resource Systems: Theory and Policy Implications*. Research Report 3. International Water Management Institute, Colombo, Sri Lanka, 15 pp.

Molden, D.J., Sakthivadivel, R., Perry, C.J., de Fraiture, C. and Kloezen, W.H. (1998) *Indicators for Comparing Performance of Irrigated Agricultural Systems*. Research Report 20, International Water Management Institute, Colombo, Sri Lanka, 26 pp.

Sarwar, A., Bastiaanssen, W.G.M., Boers, Th.M. and van Dam, J.C. (2000) Evaluating drainage design parameters for the Fourth Drainage Project, Pakistan by using SWAP model: Part 1: calibration. *Irrigation and Drainage Systems* 14, 257–280.

Tahir, Z. and Habib, Z. (2000) *Land and Water Productivity Trends Across Punjab Canal Commands*. International Water Management Institute, Working Paper 14. Pakistan Country Series No. 3, International Water Management Institute, Lahore, 35 pp.

Appendix 1: canal command wise water balances for rabi and kharif

A negative net groundwater use reveals recharge, a positive value relates to groundwater depletion. All data are expressed in gross canal command area.

	Rabi				Kharif			
Canal command area	Rain	Canal water	ET_a	Net groundwater use	Rain	Canal water	ET_a	Net groundwater use
1	26	55	346	+265	410	281	633	−58
3	36	212	336	+87	295	279	588	+15
4	25	59	320	+236	254	290	583	+39
5	25	64	347	+258	250	466	575	−141
9	25	256	367	+86	480	356	675	−161
10	25	140	359	+195	305	222	570	+43
11	44	165	300	+91	310	233	453	−90
13	25	234	350	+91	250	380	595	−35
17	25	30	302	+246	250	360	549	−61
19	25	612	222	−415	145	558	421	−282
20	25	225	277	+28	150	480	480	−150
22	25	146	363	+192	65	466	594	+64
23	25	217	344	+102	138	677	622	−193
24	25	138	335	+172	206	628	597	−237
25	25	29	347	+293	237	212	634	+184
31	25	97	391	+269	50	820	707	−163
32	25	203	372	+144	50	514	599	+35.3
33	25	254	404	+125	50	396	635	+189
34	25	120	422	+279	50	1425	720	−755
35	25	308	405	+71	50	583	597	−36
36	25	373	422	+24	50	577	697	+70
37	25	266	304	+13	50	322	500	+129
39	25	245	358	+88	127	367	619	+126
41	25	286	392	+80	150	415	756	+191
42	25	156	411	+230	120	820	790	−149
43	25	147	412	+240	58	563	776	+155